Surface Science 609 (2013) 119–128

Contents lists available at SciVerse ScienceDirect

Surface Science

journal homepage: www.elsevier.com/locate/susc

Acoustic waves in (0001) III-N and MgO/ZnO superlattices

D. Martínez-Gutiérrez, V.R. Velasco *

Instituto de Ciencia de Materiales de Madrid, CSIC, Sor Juana Inés de la Cruz 3, 28049 Madrid, Spain

ARTICLE INFO

Article history:
Received 18 July 2012
Accepted 29 November 2012
Available online 7 December 2012

Keywords:
Superlattices
Acoustic waves
Phonons

ABSTRACT

We study the acoustic waves of (0001) wurtzite MgO-ZnO and III-N superlattices. We obtain the dispersion curves as a function of the wavevector parallel to the interfaces. We consider different ranges of the thicknesses of the constituent materials forming the superlattices. Due to the transverse elastic isotropy of the basal plane of the wurtzite structure there is a decoupling of the transverse waves propagating in this plane from the coupled displacements of the sagittal waves. The dispersion curves show a qualitative picture similar in all the superlattices considered here for each of the thickness ranges studied. The sagittal waves show important differences in the dispersion curves when compared with the transverse waves. They show gaps of irregular shape not present in the transverse wave dispersion curves.

1. Introduction

III-N semiconductors have been studied quite recently as a consequence of being good candidates for applications in optoelectronics [1,2] and microelectronics [3]. These potential capabilities come from the wide range of direct bandgaps, 6.3 eV (AlN), 3.4 eV (GaN) and 0.7 eV (InN), that together with those of their ternary compounds cover the range from the infrared to the ultraviolet. In the wurtzite crystal structure, normally exhibited by these materials, there is a macroscopic polarization playing a capital role in the electrical and optical properties.

More recently the ZnO based materials are emerging as strong alternatives to the III-N. This is due to the fact that many properties of ZnO are similar to those of GaN. A very important fact, as compared to GaN, is the capability of growing ZnO single crystals [4] to be employed as substrates for the growth of thin film devices. This allows the production of high quality films by homoepitaxy and avoids the troubles with the dislocation formation due to epitaxial mismatch in GaN growth. Besides this, the ZnO bandgap (3.37 eV) [5] is quite close to that of GaN. It can also be varied in a systematic way by alloying with CdO [6] or MgO [7,8]. On the other hand CdO and MgO do not appear naturally in the wurtzite structure. Nevertheless, several experimental groups achieved the growth of ZnO/MgZnO multiple quantum wells [9–13]. It has also been found that a MgO layer can take wurtzite structure on a high-quality ZnO buffer layer when the thickness of the MgO layer is less than 10 nm [14].

Although there are no experimental values for the electronic and elastic properties of MgO in the wurtzite structure, several theoretical calculations [15,16] have provided these values.

Superlattices (SL's) are important for applications in acoustics and other areas. There is a recent and very comprehensive review on the properties of acoustic waves in layered materials [17]. Superlattices can operate as phonon mirrors and filters [18,19]. They can be employed also as acoustic cavities, where a layer with a different material or a different thickness is introduced in a finite superlattice [20,21].

Not much is known about the acoustic properties of these systems. The acoustic waves of the III-N (001) zinc-blende superlattices were studied recently [22]. It was found that for the different propagation directions, due to the elastic anisotropy of the materials, wide acoustic band gaps were present, starting at reasonably low values of κd (κ being the absolute value of the parallel wavevector and d the superlattice period).

The basal plane of the wurtzite structure has transverse elastic isotropy allowing in this case a decoupling of the motion of the transverse acoustic wave traveling in this plane from the coupled displacements of the sagittal motion along the other two axes perpendicular to the transverse motion on the plane. Thus there will be different dispersion curves and gaps for the transverse motion in the basal plane interfaces and for the sagittal components. These gaps can exist for different ranges of frequency and parallel wavevector values, thus opening, in principle, different possibilities for applications of the acoustic waves in these superlattices.

We shall study here the dispersion curves of the acoustic waves of (0001) superlattices of AlN/InN, AlN/GaN, GaN/InN and MgO/ZnO.

In Section 2 we present briefly the theoretical model and the method of calculation. Results are presented in Section 3. Conclusions are summarized in Section 4.

2. Theoretical model and method of calculation

The systems considered here are SL's formed by alternating layers of AlN/InN, AlN/GaN, GaN/InN and MgO/ZnO, respectively. A schematic

* Corresponding author.
E-mail address: vrvr@icmm.csic.es (V.R. Velasco).

0039-6028/$ – see front matter © 2012 Elsevier B.V. All rights reserved.
http://dx.doi.org/10.1016/j.susc.2012.11.013

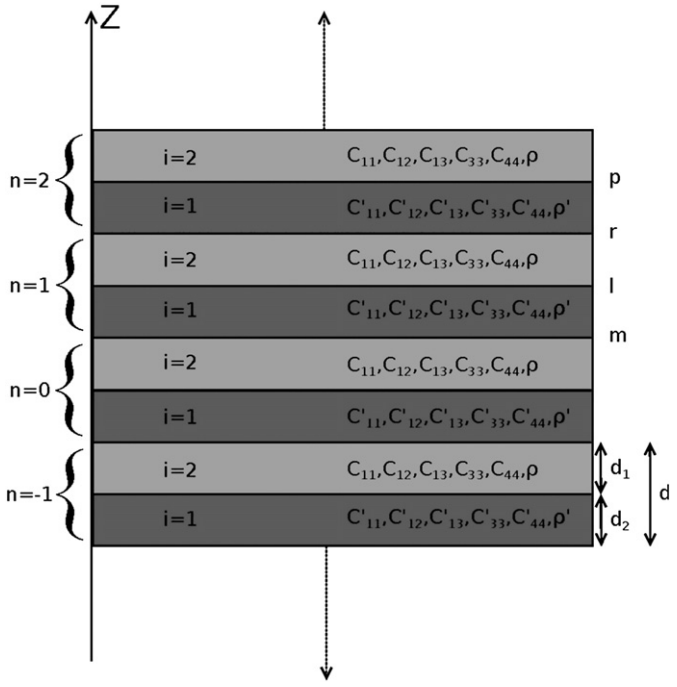

Fig. 1. Sketch of the superlattices considered in this work showing the different layers with the corresponding thicknesses, elastic constants and mass densities of the constituent materials.

view of the superlattices is given in Fig. 1. There we show the layers of the constituent materials together with their elastic coefficients, mass densities and thicknesses. The crystal axes of all the materials forming the superlattices are aligned and the interfaces are (0001) basal planes of the wurtzite structure. Taking into account the transverse elastic isotropy of the hexagonal crystals we have to consider only the absolute value κ of the parallel wavevector κ in the basal plane.

In Table 1 we give the values of the mass densities and elastic constants of the wurtzite AlN, GaN and InN [23], together with those of wurtzite ZnO [24] and MgO [15,16].

The velocities of the bulk acoustic waves propagating in the present geometry are:

$$v_{T1}^2 = \frac{C_{44}}{\rho}, v_{T2}^2 = \frac{C_{66}}{\rho}, v_L^2 = \frac{C_{11}}{\rho}, \tag{1}$$

In the present case we have two different transverse wave velocities.

In Table 2 we give the velocities of the acoustic waves of the materials considered in Table 1. We can see that $v_{T1} > v_{T2}$ in all materials, except MgO, whose elastic data are obtained from theoretical calculations. It is seen that AlN has the highest velocity values for the different elastic waves of all the materials considered here.

Table 2
Velocities of the acoustic waves for AlN, GaN, InN, MgO[(a)] [15], MgO[(b)] [16] and ZnO, calculated with the data of Table 1.

Material	$v_{T1}(10^3\ \mathrm{ms}^{-1})$	$v_{T2}(10^3\ \mathrm{ms}^{-1})$	$v_L(10^3\ \mathrm{ms}^{-1})$
AlN	6.307	5.970	11.030
GaN	4.463	4.132	7.963
InN	2.816	2.655	5.722
MgO[(a)]	4.294	5.416	7.875
MgO[(b)]	3.547	4.060	7.372
ZnO	2.811	2.753	6.116

To obtain the dispersion curves of the acoustic waves in the superlattices we employ the Surface Green Function Matching (SGFM) method [25] which is very adequate to study the properties of multi-layer systems formed by anisotropic materials [26]. We shall give here the detailed expression for the Green's function and normal derivatives particular to the hexagonal system together with the essential formal expressions for the study of the superlattices. The formal and practical details can be found in [25].

The bulk material Green's function **G** for hexagonal crystals is given by

$$\mathbf{G} = \begin{bmatrix} \frac{C_{33}k_z^2 + \left(C_{44}\kappa^2 - \rho\omega^2\right)}{C_{33}C_{44}\left(\beta_1^2 + k_z^2\right)\left(\beta_2^2 + k_z^2\right)} & 0 & -\frac{(C_{44}+C_{13})\kappa k_z}{C_{33}C_{44}\left(\beta_1^2 + k_z^2\right)\left(\beta_2^2 + k_z^2\right)} \\ 0 & \frac{1}{C_{44}\left(\beta_t^2 + k_z^2\right)} & 0 \\ -\frac{(C_{44}+C_{13})\kappa k_z}{C_{33}C_{44}\left(\beta_1^2 + k_z^2\right)\left(\beta_2^2 + k_z^2\right)} & 0 & \frac{C_{44}k_z^2 + \left(C_{11}\kappa^2 - \rho\omega^2\right)}{C_{33}C_{44}\left(\beta_1^2 + k_z^2\right)\left(\beta_2^2 + k_z^2\right)} \end{bmatrix}, \tag{2}$$

where

$$\beta_1^2 = \frac{1}{2}\left[B + \left(B^2 - 4C^2\right)^{\frac{1}{2}}\right], \tag{3}$$

$$\beta_2^2 = \frac{1}{2}\left[B - \left(B^2 - 4C^2\right)^{\frac{1}{2}}\right], \tag{4}$$

$$B = \frac{1}{C_{33}C_{44}}\left[\left(C_{44}^2 + C_{11}C_{33}\right)\kappa^2 - (C_{13}+C_{44})^2\kappa^2 - (C_{33}+C_{44})\rho\omega^2\right], \tag{5}$$

$$C^2 = \frac{1}{C_{33}C_{44}}\left(C_{44}\kappa^2 - \rho\omega^2\right)\left(C_{11}\kappa^2 - \rho\omega^2\right), \tag{6}$$

$$\beta_t = \left(\frac{C_{11}-C_{12}}{2C_{44}}\kappa^2 - \frac{\rho\omega^2}{C_{44}}\right)^{\frac{1}{2}} = \left(\frac{C_{66}}{C_{44}}\kappa^2 - \frac{\rho\omega^2}{C_{44}}\right)^{\frac{1}{2}}, \tag{7}$$

(In all cases $\mathrm{Re}(\beta_i) > 0$, $\mathrm{Im}(\beta_i) > 0$, $i = 1,2,t$.)

The surface projected elements of the Green function are obtained from

$$G_{ij}\left(\kappa, \omega^2\right) = \lim_{\epsilon \to 0} \frac{1}{2\pi} \int_{-\infty}^{\infty} \exp[i\epsilon k_z] G_{ij}\left(\kappa, k_z; \omega^2\right) dk_z, \tag{8}$$

Table 1
Elastic constants for AlN, GaN and InN [23], elastic constants for MgO[(a)] [15], MgO[(b)] [16], ZnO [24] and mass densities employed in our calculations.

Material	$C_{11}(10^{10}\ \mathrm{Nm}^{-2})$	$C_{12}(10^{10}\ \mathrm{Nm}^{-2})$	$C_{13}(10^{10}\ \mathrm{Nm}^{-2})$	$C_{33}(10^{10}\ \mathrm{Nm}^{-2})$	$C_{44}(10^{10}\ \mathrm{N\,m}^{-2})$	$\rho(10^3\ \mathrm{kg\ m}^{-3})$
AlN	39.6	13.7	10.8	37.3	11.6	3.255
GaN	39.0	14.5	10.6	39.8	10.5	6.15
InN	22.3	11.5	9.2	22.4	4.8	6.81
MgO[(a)]	22.2	9.0	5.8	10.9	10.5	3.58
MgO[(b)]	19.46	10.45	9.99	11.96	5.9	3.58
ZnO	20.97	12.11	10.51	21.09	4.25	5.606